Brain Tumor Segmentation Using OTSU Embedded Adaptive Particle Swarm Optimization Method and Convolutional Neural Network

Surbhi Vijh, Shilpi Sharma and Prashant Gaurav

Abstract Medical imaging and deep learning have tremendously shown improvement in research field of brain tumor segmentation. Data visualization and exploration plays important role in developing robust computer aided diagnosis system. The analysis is performed in proposed work to provide automation in brain tumor segmentation. The adaptive particle swarm optimization along with OTSU is contributed to determine the optimal threshold value. Anisotropic diffusion filtering is applied on brain MRI to remove the noise and improving the image quality. The extracted features provided as data for training the convolutional neural network and performing classification. The proposed research achieves higher accuracy of 98% which is better over existing methods.

Keywords Brain tumor · Segmentation · Adaptive particle swarm optimization · Deep learning · Deep neural network · Convolutional neural network

1 Introduction

Artificial intelligence and computer vision are showing remarkable improvement in development of automatic medical diagnosis system. According to National Brain Tumor Society, it is estimated that 78,980 new cases are predicted in 2018 in the United States. Cancer has been observed and considered as the disease that may

S. Vijh
Department of Information Technology, KIET group of Institutions, Ghaziabad, India
e-mail: surbhivijh428@gmail.com

S. Sharma (✉) · P. Gaurav
Department of Computer Science and Engineering, Amity School of Engineering and Technology, Amity University Uttar Pradesh, Sector 125, Noida, India
e-mail: ssharma22@amity.edu

P. Gaurav
e-mail: prashantgaurav36@gmail.com

J. Hemanth et al. (eds.), *Data Visualization and Knowledge Engineering*,
Lecture Notes on Data Engineering and Communications Technologies 32,
https://doi.org/10.1007/978-3-030-25797-2_8

cause maximum death around the world as it is difficult to perform diagnosis of patient. The Brain cancerous tumor can broadly be classified [1] into primary tumor and secondary tumor (metastatic tumor). Image processing techniques [2] are applied in detection and exploring the abnormalities issues in tumor detection. The early stage of detection can improve the process of decision making by radiologist, physician, experts and can increase the survival rate of Tumor patients. The automatic computer aided diagnosis system is proposed in medical imaging with the usage of deep learning. Brain tumor occurs due to the presence of abnormality as the cell divides and its growth increase. The different modalities of Magnetic resonance imaging are present such as T1-weighted MRI, T2-weighted MRI, Flair and Flair with contrast enhancement. The segmentation of the brain tumor MRI is the most challenging task in contributing towards the development of diagnosed system [3]. A new approach is proposed in construction of automatic diagnosis system. The simulated steps performed in proposed system are (a) image acquisition (b) pre-processing (c) segmentation (d) post processing (e) feature extraction (f) classification. There are various segmentation [4] approaches used previously such as region growing technique, Thresholding, clustering, edge detection etc. In the proposed work, the novel hybrid approach of OTSU and adaptive particle swarm optimization is adopted along with convolutional neural network. Nature inspired metaheuristic optimization algorithm are used for optimizing the problem by resembling the physical or biological phenomenon. In computer science, there are various metaheuristic optimization technique such whale optimization algorithm [5], Particle swarm optimization [6], Adaptive PSO, Ant bee colony [7], Ant colony optimization (ACO), cuckoo search [8]. The adaptive particle swarm optimization technique is implemented because of improved time and space performance. The OSTU + APSO approach is providing the optimal threshold value which enables to perform the segmentation in improved manner. Anisotropic diffusion filtering is applied for smoothing and denoising the brain MRI. Feature extraction is performed with the usage of GLCM technique in which all statistical and texture characteristics are extracted. The data organized in feature extraction stage is used for training and testing of convolutional neural network for classification. The classification is performed to predict whether the tumor is present or not. Deep neural network considers the selection of network structure, activation function, number of neurons, learning rate and other factors which are highly dependent on data representation [9]. Convolutional neural network contributing towards the medical imaging data visualization, analyzation and exploration of large amount of data. Convolutional neural network enables to design the computer aided diagnosis system with higher accuracy in medical image domain [10]. The performance of the developed automatic computer diagnosis system is measured through parameter accuracy. The accuracy obtained of proposed system is 98% which is better than any other existing system.

The proposed paper is organized into different section in which Sect. 2 describes regarding literature review and its related work, Sect. 3 represents the proposed methodology and contribution towards the paper, Sect. 4 presents the simulated experimental results, Sect. 5 describes related to result and its discussion, Sect. 6 states the conclusion and future scope of the proposed work.

2 Literature Review

In recent years, the research in medical imaging is increasing exponentially to show advancement in data visualization and improving the survival rate of patients at early stage. The objective of researchers is to develop the robust computer aided automatic diagnosis system for detection of brain tumor. The emerged growing technique known as deep learning is contributing to pattern recognition, artificial intelligence, machine learning applications [11–13]. The computational architecture containing multiple processing layers are trained to acknowledge the data visualization and its various representation [14]. Convolution neural network is considered promising method in fields of computer vision, various application of medical imaging analysis and natural language processing. The deep learning techniques helps in providing effective improved performance and approaches [15, 16]. Medical diagnosis is the most challenging decision-making process. The fundamental procedure of artificial intelligence helps the radiologist and experts in taking decision regarding the process of treatment [17, 18]. The deep learning outperforms in handling the immense data images and the multiple layer of abstraction. The convolutional neural network can be used to determine wider range of perceptual task and object recognition [19].

There are numerous technique which are used to obtain information of human organ among which MRI is desired non-invasive method used to evaluate the neural activity of human brain [20]. MRI was invented in 1970 considered as medical imaging technique providing the internal details as well essential information of irregularity and contrast changes in human soft tissue [21]. The magnetic properties of tissues are observed using magnetic field, radio waves of MRI scanners and produces the images having structural analysis of human body. Magnetic resonance imaging lead emphasis on visualization of tissues accommodating hydrogen such as Cerebrospinal fluid (CSF), brain, bone marrow etc. The MRI images are interpreted and analyzed by radiologist, experts, physician to detect and screen the abnormality present in brain [22]. Neoplasm (tumor) are broadly structured into three types (a) Benign (b) Pre-malignant (c) Malignant [23].

Medical image processing has become very efficient technique for treatment of cancer patient and detection of tumor. Brain Tumor segmentation [24] are broadly classified into three categories (a) manual (b) semiautomatic (d) fully automatic. The manual segmentation is performed by radiologist and experts which provides time consuming and poor outcomes. Thus, semiautomatic is introduced in which human know few parameters on basis of which analyzation is performed. It provided better results than manual segmentation. However, fully automatic segmentation system is emerged as booming technique which outperforms and works on the basis of prior information using the concept of artificial intelligence. The different modalities of tumored brain MRI shown in Fig. 1.

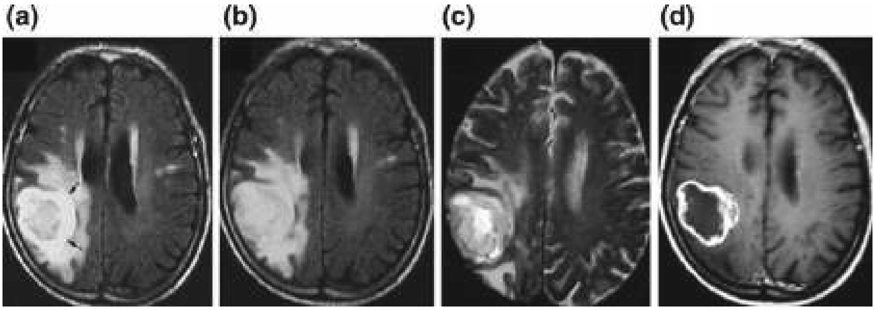

Fig. 1 **a** T1-weighted MRI **b** T2-weighted MRI **c** Flair **d** Flair with contrast enhancement

Image segmentation of brain magnetic resonance imaging considered as difficult and important process for detection of brain tumor and extracting the important features for determining the abnormalities present [21]. It is very difficult task needed to be performed since the abnormal image holds various irregularities in shape, structure and size and location [25]. The selection of right segmentation technique helps to perform skull stripping of brain MRI. The skull stripping is used to remove the cerebellum tissues on different modalities of images such as T1 weighted and T2 weighted magnetic resonance image in various medical applications [26, 27]. Patel et al. [28] presented different segmentation techniques for studying the detection of brain tumor named as (a) edge-based method (b) Region growing [29] (c) clustering method (d) Fuzzy c-mean clustering [30] (e) Thresholding. Cabria et al. [31] proposed a new technique for segmentation named as fusion of potential field clustering and another ensemble method. The methodology is applied on BRATS MRI benchmark for detection of tumor region. Ayachi et al. [32] developed automatic computer aided diagnosis system for brain tumor segmentation. The pixel classification segmentation technique is applied and the system involves support vector machine for classification Gliomas dataset. Soleimani et al. [33] proposed methodology in which ant colony optimization technique is considered for determining brain tumor segmentation and improving the accuracy. The usage of metaheuristic techniques in development of diagnosis system helps to obtain optimized threshold value of parameters. Jothi et at [34] stated a novel approach for optimal feature selection of brain MRI using firefly based quick reduct and tolerance rough set. Manic et al. [35] implemented the multilevel thresholding based upon firefly algorithm to segment the gray scale image by using kapur/Tsallis entropy to find optimal threshold of image and then performance is computed on parameters such as root mean squared error, Normalized absolute error, Structural Similarity Index Matrix, Peak signal to noise ratio (PSSR). Sharma et al. [36] proposed a methodology in which statistical features of MRI brain image are extracted using GLCM. The k-mean and ANN model is created using the extracted information for determining the performance parameters.

Jafari et al. [37] presented a novel approach for developing automatic tumor detection system of brain and classifying whether brain image is normal or abnormal. The genetic algorithm is implemented for considering the selected optimal features. The classification technique used for detection is support vector machine achieving accuracy up to 83.22%. Jiang et al. [38] presented the medical image analysis and characterization with the usage of intelligent computing. The medical image segmentation and edge detection are formulated with the support of different artificial neural network models such as feedforward neural network, feedback neural network, self-organizing maps to obtain the medical image analysis. They are shown the various application where ANN can be used extensively such as in tumor tracking [39], image compression [40] and enhancement [41].

Havaei et al. [42] proposed a methodology for automatic brain tumor segmentation of glioblastomas MRI using deep learning. The various convolutional neural network architecture is designed among which fully connected CNN is used for determining the analysis on BRATS (2013) testing dataset. It is evaluated and observed that the proposed methodology was providing improved accuracy, speed over traditional methods in computer vision. Gao et al. [43] stated a novel approach by considering the brain CT images to perform classification by using deep learning techniques. The diagnosis computer aided system is developed for predicting the Alzheimer's disease. They partitioned the dataset into three parts AD, lesion and normal ageing and predicted the classification using 2D and 3D CNN networks architecture. The average of 87.6% of accuracy is obtained for the categorized structure of images.

Pereira et al. [44] performed automatic segmentation of brain tumor in MRI images by considering BRATS 2013 And BRATS 2015 dataset. The technique used is convolutional neural network for data visualization and analysis. The system is validated using BRATS 2013 database and acquired first position in dice similarity coefficient matrix for the target dataset. Sharma et al. [45] designed a methodology using differential evolution embedded OTSU and artificial neural network for the automatic segmentation of brain tumor. The brain MRI of 58 patients are considered for evaluating the performance parameters. The accuracy of proposed system obtained is of 94.73%.

Mohan et al. [46] showed the analysis on medical image of brain tumor magnetic resonance imaging and its grade classification is performed. The hybrid approach of image processing, machine learning and artificial intelligence is used to improve the accuracy of diagnosis system. The methodology involves extraction and performing grading of tumor. Chen et al. [47] proposed a novel approach of segmentation on 3D MR image of brain and used Voxel wise residual network (VoxResNet) of deep learning to obtain volumetric performance information of image. Zhao et al. [48] presented brain tumor segmentation model with the usage of hybrid network of fully connected convolutional network and conditional random fields. Deep learning is used for improving the system robustness. The different modalities of brain MRI is considered such as T1, T2, flair constant of BRATS 2013, BRATS 2015. BRATS 2016 segmentation challenge. The analysis of previous literature and their techniques performance are shown in Table 1.

Table 1 Analysis of related paper

Author	Segmentation technique	Classifier	Performance	Dataset
Kumar et al. [49]	Gradient vector flow—boundary based technique	PCA-ANN	95.37%	55 patient-T1 weighted MR
Lashkari et al. [50]	Histogram equalization morphological operation	MLP model-ANN	98%	210 case-T1 weighted, T2 weighted MRI
Wang et al. [51]	_	Cascaded CNN model anisotropic CNN model	_	BRATS 2017
Byale et al. [52]	K-mean segmentation, GMM segmentation	Artificial neural network	93.33%	60 sample MRI
Kharrat et al. [53]	_	GA + SVM	94.44%	83 sample images—T2 weighted
Sharma et al. [37, 46]	Global thresholding, Anisotropic diffusion filtering	DE + ANN	94.34%	T1 weighted MRI
Ortiz et al. [54]	SOM clustering algorithm	_	_	IBSR
Shanthi et al. [55]	Fuzzy c-mean algorithm	ANN	_	_
El Abbadi et al. [56]	Morphological operations	Probabilistic neural network	98%	65 MR image dataset
El-Dahshan et al. [57]	_	FP-ANN	97%	70 MR images

Deep learning consists of multiprocessing layers which can handle larger complex hierarchy of data [58]. Deep artificial neural network is applied in numerous medical visualization analysis as it shows outstanding performance efficiency in comparison to other manual or semi-automatic techniques [59]. There are various deep learning algorithms such as deep Boltzmann machine, Stack auto-encoders, Convolutional neural network, fine tuning deep models for target task [60] etc. The CNN architecture involves many layers of pooling, activation and classification. The different CNN architecture used and their performance are discussed in Table 2.

Table 2 CNN techniques and its analysis

Author	Data	CNN model	Performance
Kamnitsas et al. [61]	BRATS 2015	Patch-wise CNN	DSC (0.9) (complete)
Zhao et al. [62]	BRATS 2013	Patch-wise CNN	Accuracy (0.81) (overall)
Nie et al. [63]	Private data	Semantic-wise CNN	DSC 85.5%(CSF)
Li et al. [64]	ILD	Single convolution layer	Accuracy (0.85) (overall)
Chao et al. [65]	MNIST	CaRENets	Accuracy (0.925) (overall)

3 Proposed Methodology

The steps for proposed study and contribution for development of automatic brain tumor segmentation system is shown as follows.

(a) The 61 sample cases of T1-weighted brain magnetic resonance images are obtained from IBSR (Brain segmentation repository). The 40 MS-free data sample images taken from Institute of neurology and genetics, at Nicosia Cyprus [66] and Laboratory of eHealth at the University of Cyprus [67]. The obtained images are normalized so that segmentation could be applied efficiently and properly.

(b) The skull stripping is essential fundamental process desired for segmentation and analysis of brain tumor MRI [68]. It is considered as important pre-processing phase for removing the non-cerebral tissue and plays role in clinical research of neuroimage applications [69]. In the proposed method, the new hybrid approach of adaptive particle swarm optimization [70, 71] and OTSU [29] are contributed to paper for performing improved skull stripping of brain. The hybridization is providing the optimized threshold value which improves the efficiency and reliability of system. The process flow of skull stripping is described as follows:

   (i) After normalization of dataset, the Gaussian filter is applied for smoothing of image and removing the noise. The mathematical formulation of gaussian filter can be shown as

$$\mathrm{G(a, b)} = \frac{1}{2\pi\sigma^2} e^{-\frac{z}{2\pi\sigma^2}} \tag{1}$$

$$\mathrm{Z} = a^2 + b^2 \tag{2}$$

a represents the distance on x axis and b represents the distance on y-axis from origin, σ represents the standard deviation of gaussian distribution.

(ii) The evaluation of adaptive thresholding with the usage of intensity histogram. Adaptive thresholding is dynamic process of obtaining threshold value which would be dependent upon the neighboring pixels intensity.

(iii) Calculate the threshold value through hybrid approach of OSTU + APSO. This is providing excellent results when compared to other methods. The modified particle swarm optimization introduces two additional adaptive parameters to improve convergence speed named as adaptive factor, perturbation factor. The fitness function value is obtained by applying metaheuristic algorithm.

(iv) Morphological operation performs functions in relevance to shape and size of image. The structuring element is taken as input for extracting the useful features and representation of data. The four elementary mathematical operations of morphology in image processing can be represented

$$\text{Erosion}: \ \mathrm{C} \ominus \mathrm{D} = \{B|(D)_B \subseteq \mathrm{C}\} \tag{4}$$

$$\text{Dilation}: \ \mathrm{C} \oplus \mathrm{D} = \{B|(D)_B \cap C \neq \emptyset\} \tag{5}$$

$$\text{Opening}: \ \mathrm{C} \ominus \mathrm{D} = \mathrm{C} \ominus \mathrm{D} \oplus \mathrm{D} \tag{6}$$

$$\text{Closing}: \ \mathrm{C} \ominus \mathrm{D} = \mathrm{C} \oplus \mathrm{D} \oplus \mathrm{D} \tag{7}$$

(v) The skull stripping is performed by keeping the extracted mask on input image so that extra cerebral tissue can be eliminated and region of interest can be proceeded for further operations.

(c) The denoising popular technique for brain MRI known as Anisotropic diffusion filtering is performed to improve the quality of extracted brain MRI by intensify the contrast between the regions. It is type of enhancement method to balance the different noise levels in image.

(d) Feature extraction is the most crucial step for evaluation of various parameters of image. On the basis of extracted features, the performance predictions and calculation could be obtained. In the proposed work, the 19 statistical and texture related parameters are extracted so that efficient system could be developed. GLCM method is used for extracting the features. GLCM (grey level co-occurrence matrix) is statistical method considering the spatial relationship of pixels. The 19 statistical features obtained in proposed work are autocorrela-

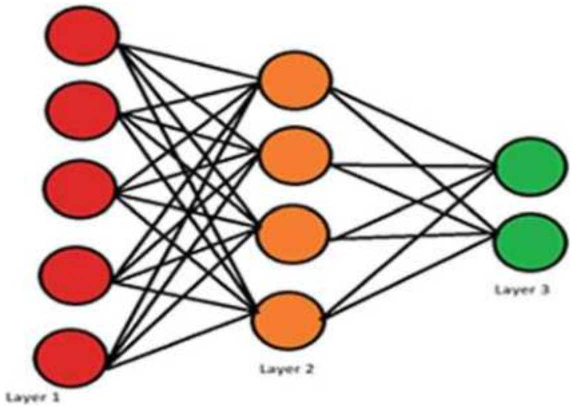

Fig. 2 Fully connected CNN

tion, cluster prominence, cluster shade, contrast, correlation, entropy, variance, dissimilarity, energy, difference Entropy, homogeneity, information measure of correlation 1, information measure of correlation 2, inverse difference, maximum probability, sum average, sum entropy, sum of square variance, sum variance. The extracted features are given as input to convolutional neural network so that tumor classification can be determined.

(e) Convolutional neural network is used as classification model for tumor detection system. The CNN outperforms in comparison to other classifiers if tremendous amount of data is needed to be handled. In the proposed work the three layers of convolutional neural network which uses activation function. The layer 1 and layer 2 uses [72] RELu activation function and layer 3 uses SoftMax activation function. The data is divided into 7:3 ratio. The layers are densely connected from one neuron to another neuron. The 98% of accuracy is achieved in proposed work. The diagrammatic representation is shown in Fig. 2.

The representation of procedural flow diagram of the proposed algorithm is represented in Fig. 3.

The proposed model algorithm steps are shown in table and are implemented on MATLAB R2018b

4 Experimental Results

4.1 Simulated Results

The proposed work uses 101 sample images of brain MRI. The 70% of data are used in training and 30% of data are used in testing. There are 61 sample case images of tumored IBSR dataset and 40 sample images of non-tumor MS-free brain

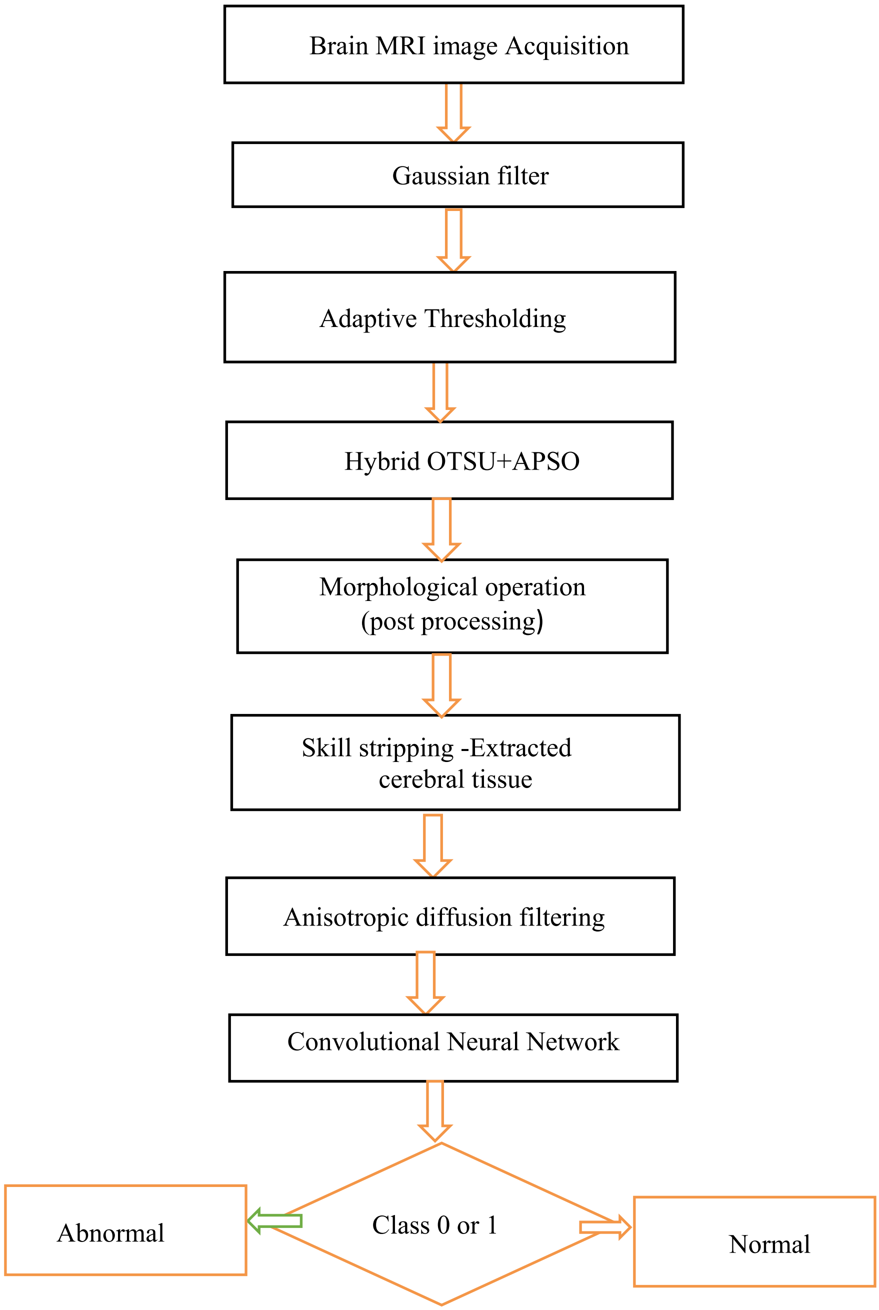

Fig. 3 Flow diagram of proposed model

MRI dataset. The adopted methodology performs hybridization of OTSU + APSO to determine optimal threshold value to obtain segmentation. The 19 features are extracted using GLCM (grey scale level matrix) which are used for training purpose in convolutional neural network. The 3 layers of convolutional neural network are densely connected to each other.

An example of IBSR tumored MRI are shown in figure (i) Normalize Image (ii) Gaussian Filter (iii) OTSU Thresholding + APSO (iv) and (v) Mathematical Morphology (vi) Skull Stripped Image (vii) Anisotropic Diffusion Filtering (viii) GLCM

An example of MS-free dataset non tumored MRI are shown in Fig. 4. (i) Normalize Image (ii) Gaussian Filter (iii) OTSU Thresholding + APSO (iv) and (v)

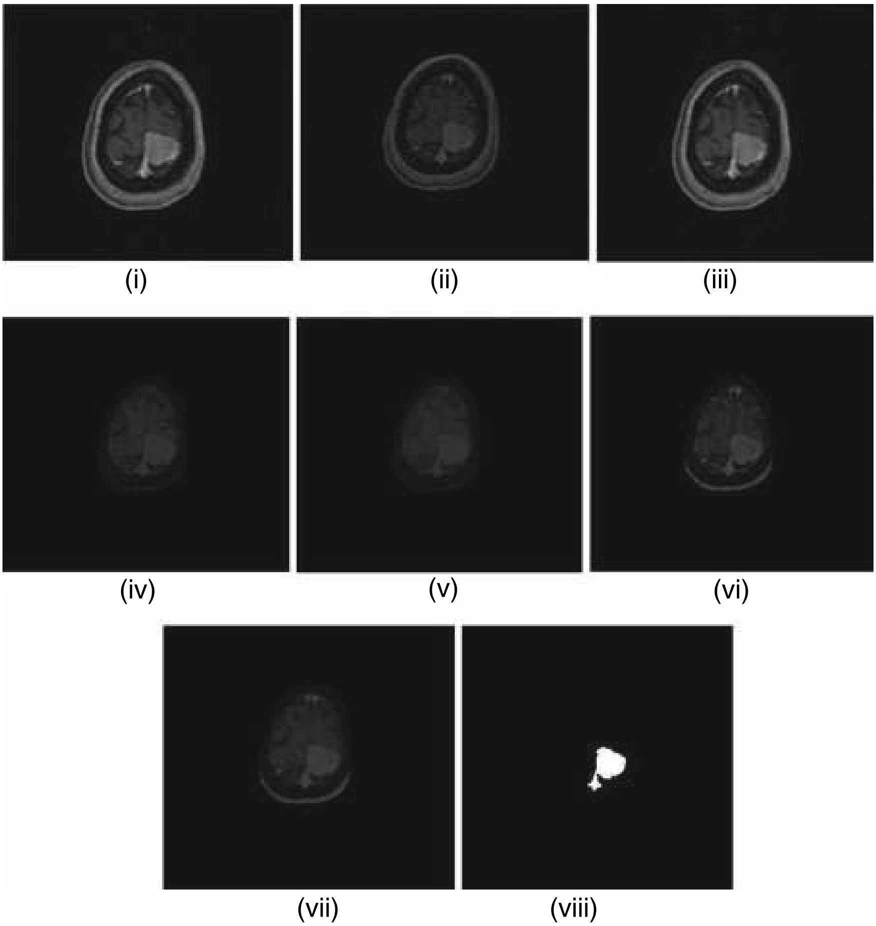

Fig. 4 Tumored images

Mathematical Morphology (vi) Skull Stripped Image (vii) Anisotropic Diffusion Filtering (viii) GLCM

The Table 4 represents the average fitness value and the segmented image quality metrics [73, 74] are calculated using peak signal to noise ratio (PSNR), structural similarity index matrix (SSIM) and Dice similarity parameter. The example outcomes of IBSR and MS-free dataset are shown from 1–25 to 26–40.

The mathematical formulation of few parameters of GLCM [75–77] technique are presented. All parameters are calculated for every sample MRI image of patients and the evaluation of parameters are independent of each other.

- Energy $= \sum_{i,j=0}^{L-1} \left(k_{i,j}\right)^2$ (8)
- Entropy $= \sum_{i,j=0}^{L-1} -\lg\left(k_{i,j}\right)k_{i,j}$ (9)
- Contrast $= \sum_{i,j=0}^{L-1} k_{i,j}(i-j)^2$ (10)
- Homogeneity $= \sum_{i,j=0}^{L-1} \frac{\left(k_{i,j}\right)}{1+(i-j)^2}$ (11)
- Correlation $= \sum_{i,j=0}^{L-1} \left(k_{i,j}\right) \cdot \frac{(i-\mu)(j-\mu)}{(\sigma)^2}$ (12)
- Standard deviation $= \sqrt{\sum_{i,j=0}^{L-1} k_{i,j}(i-\mu)^2}$ (13)
- Shade feature $= \mathrm{sgn(C)}|C|^{1/3}$ (14)

sgn represents the sign of real number which can be positive, negative

$$\mathrm{C} = \sum_{i,j=0}^{L-1} \frac{Ki,j(i+j-2\mu)^3}{(\sigma)^3\left(\sqrt{2(1+C)}\right)^3} \quad (15)$$

- $(k_{i,j})$ = represents the attributes i, j of normalized symmetric matrix of GLCM
- L = Number of levels
- μ represents mean of GLCM and can be formulated as

$$\mu = \sum_{i,j=0}^{L-1} \sum_{i,j=0}^{L-1} \mathrm{i}k_{i,j} \quad (16)$$

- $(\sigma)^2$ represents the variance of all pixels.

$$(\sigma)^2 = \sum_{i,j=0}^{L-1} k_{i,j}(i-\mu)^2 \tag{17}$$

The training and testing data are evaluated on x axis and y axis in which x-axis represents the data with class label and y axis represents the data of encoded class labels. The three layers are considered having 38 neurons in 1st layer, 19 neurons in 2nd layer and class labels in 3rd layer. The categorial cross entropy loss function of deep learning is implemented. The values considered for the neural network measures are shown as follows:

learning rate = 0.001, $\beta_1 = 0.9$, $\beta_2 = 0.999$, activation function = RELu and SoftMax

The accuracy of intelligent automatic brain tumor segmentation achieved is 98% and the loss function is 4% as presented in Table 7.

5 Results and Discussion

In the proposed study, Fig. 2 shows representation of fully connected neural network. The three layers are creating densely nested network which are aiming to provide classification results. The proceeding Fig. 3 presents the flow process of methodologies adopted and implemented. Table 3 contributes the proposed hybrid OTSU + APSO approach for obtaining the optimal or best threshold value for separating the cerebral tissue of brain and providing improved segmentation results. The Figs. 4 and 5 shows the simulated result of segmentation process. Further the Table 4 provides the mathematical measures of fitness value, PSNR, SSIM, Dice similarity. PSNR

Table 3 Hybrid algorithm of OTSU and APSO

Hybridization of OTSU + APSO for skull stripping and segmentation of MRI
1. Normalization of acquired image dataset of brain MRI 2. Skull stripping is applied to remove the cerebellum part and improving the segmentation efficiency 3. Apply anisotropic diffusion for smoothing of image 4. Feature extraction by using GLCM technique 5. Training the convolutional neural network 6. Testing the convolutional neural network to achieve the accuracy and measuring the performance

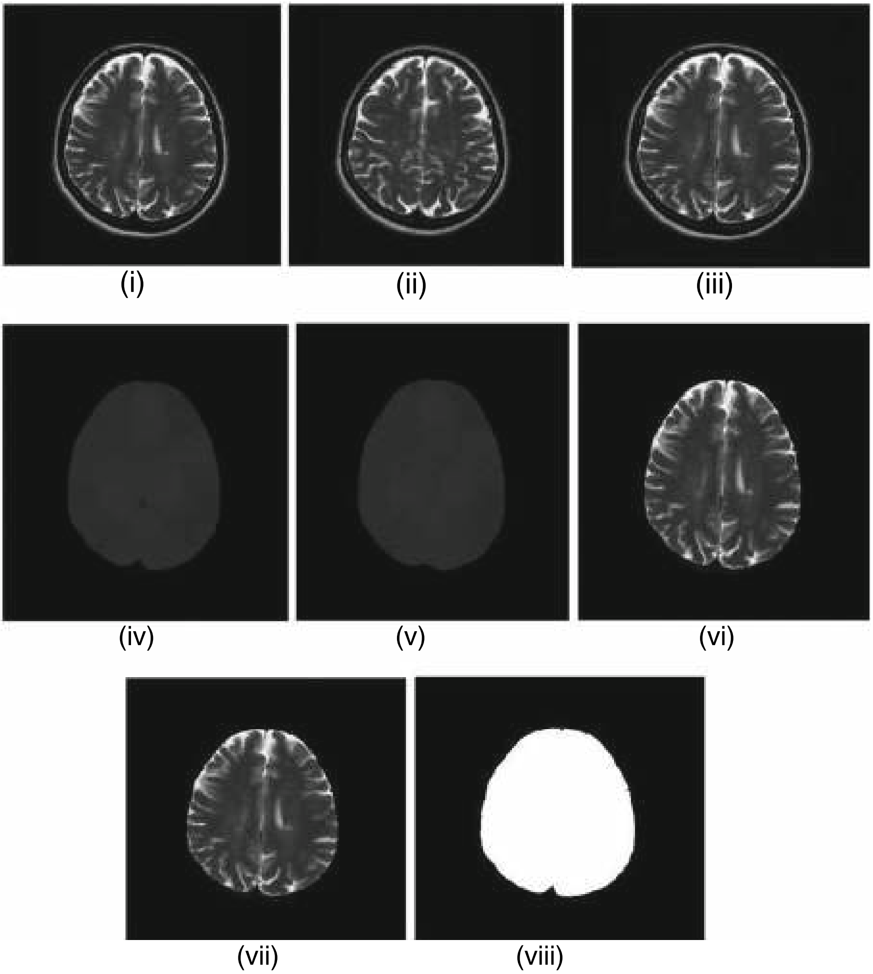

Fig. 5 Non tumored images

(peak signal to noise ratio) and SSIM determines the pixel difference and structural similarity quality metrics of segmented images. Dice similarity is statistic for evaluating the comparison of similarity between two images. The features extracted are

Table 4 Fitness values, PSNR, SSIM, Dice

Brain MRI	Fitness function value	PSNR	SSIM	Dice
Image 1	1.9913	45.7672	0.95441	0.98187
Image 2	1.9759	46.6009	0.95661	0.98443
Image 3	1.5481	46.8406	0.9566	0.98334
Image 4	1.9238	45.8822	0.9547	0.98435
Image 5	1.9751	45.9853	0.9554	0.98574
Image 6	1.9238	46.1083	0.9555	0.98439
Image 7	1.3843	46.2206	0.95593	0.98572
Image 8	1.8699	46.4003	0.95652	0.9855
Image 9	1.7917	46.6009	0.95661	0.98443
Image 10	1.0578	46.8304	0.9566	0.98334
Image 11	1.2111	45.7312	0.94363	0.9821
Image 12	1.9254	45.7589	0.94236	0.98205
Image 13	1.7899	45.8375	0.94208	0.98058
Image 14	1.7602	45.8722	0.94302	0.97993
Image 15	1.4607	45.8994	0.94247	0.98108
Image 16	1.6586	46.0584	0.941	0.98131
Image 17	1.586	46.1354	0.9399	0.97966
Image 18	1.6273	46.1821	0.93947	0.98021
Image 19	1.5251	46.2122	0.93956	0.98166
Image 20	1.897	46.3931	0.93939	0.98179
Image 21	1.1762	45.9448	0.98676	0.98639
Image 22	1.1409	45.7425	0.98918	0.98894
Image 23	1.8063	45.7003	0.98878	0.988
Image 24	1.9803	45.7184	0.98868	0.98867
Image 25	1.9913	45.7512	0.9879	0.98763
Image 26	1.6546	45.7907	0.98763	0.9875
Image 27	1.7807	45.8117	0.98747	0.98726
Image 28	1.8016	45.8636	0.98754	0.98687
Image 29	1.9627	45.4119	0.99608	1
Image 30	1.3021	45.6417	0.99591	1
Image 31	1.7973	46.1975	0.99614	1

(continued)

Table 4 (continued)

Brain MRI	Fitness function value	PSNR	SSIM	Dice
Image 32	1.4855	44.8914	0.99657	1
Image 33	1.8717	44.7648	0.99656	1
Image 34	1.794	44.7566	0.99655	1
Image 35	1.3735	44.7642	0.99655	1
Image 36	1.6309	44.8036	0.99653	1
Image 37	1.9422	44.8494	0.99649	1
Image 38	1.4554	44.9225	0.99642	1
Image 39	1.5642	45.0488	0.99633	1
Image 40	1.465	45.5681	0.99328	1
Image 41	1.8631	44.5622	0.99445	1
Image 42	1.4802	44.562	0.99443	1
Image 43	1.8498	44.5782	0.99441	1
Image 44	1.7799	44.6284	0.99433	1

provided as input for training the convolutional neural network. The Tables 5 and 6 represents the 19 features extracted from IBSR and MS-free dataset. The final parametric result of 101 sample images are shown in Table 7. It shows that proposed system achieves higher accuracy of 98%.

Table 5 Feature extraction of IBSR dataset

Sl. no.	Autocorrelation	Cluster prominence	Cluster shade	Contrast	Correlation	Difference entropy	Difference variance	Dissimilarity	Energy
1	1.0366	0.1692	0.0875	0.0039	0.8456	0.0256	0.0039	0.0039	0.971
2	1.0129	0.0649	0.0329	0.000613	0.93	0.0051	0.0006124	0.0006128	0.991
3	1.0211	0.106	0.0537	0.000766	0.9461	0.0063	0.0007653	0.0007659	0.985
4	1.0193	0.0946	0.0482	0.0013	0.9003	0.0101	0.0013	0.0013	0.986
5	1.0207	0.1016	0.0518	0.0013	0.9047	0.0103	0.0013	0.0013	0.985
6	1.0267	0.1285	0.0658	0.002	0.8893	0.0146	0.002	0.002	0.98
7	1.0273	0.1352	0.0688	0.0012	0.9367	0.009	0.0012	0.0012	0.98
8	1.1426	0.5984	0.3162	0.0066	0.9282	0.04	0.0066	0.0066	0.901
9	1.0612	0.2773	0.1441	0.0055	0.8692	0.0339	0.0054	0.0055	0.953
10	1.0612	0.2773	0.1441	0.0055	0.8692	0.0339	0.0054	0.0055	0.953
11	1.0542	0.2518	0.13	0.004	0.8924	0.0258	0.0039	0.004	0.959
12	1.046	0.2131	0.1101	0.004	0.8715	0.0263	0.004	0.004	0.965
13	1.0448	0.2075	0.1073	0.0041	0.8665	0.0267	0.0041	0.0041	0.965
14	1.0531	0.2461	0.1272	0.0041	0.8855	0.0268	0.0041	0.0041	0.96
15	1.0766	0.3429	0.1786	0.006	0.8838	0.0367	0.006	0.006	0.942
16	1.0494	0.2312	0.1192	0.0036	0.8923	0.0239	0.0036	0.0036	0.963
17	1.0271	0.1353	0.0687	0.000919	0.9495	0.0073	0.0009183	0.0009191	0.981
18	1.0278	0.1375	0.07	0.0012	0.9347	0.0094	0.0012	0.0012	0.98
19	1.0247	0.12	0.0613	0.0017	0.9001	0.0124	0.0017	0.0017	0.982
20	1.0284	0.1385	0.0707	0.0017	0.9141	0.0122	0.0017	0.0017	0.979

(continued)

Table 5 (continued)

Sl. no.	Entropy	Homogeneity	Information measure of correlation 1	Information measure of correlation 2	Inverse difference	Maximum probability	Sum average	Sum entropy	Sum of squares variance	Sum variance
1	0.0884	0.998	– 0.7144	0.306	0.998	0.9852	2.0257	0.0857	0.0127	0.0469
2	0.0321	0.9997	– 0.8621	0.218	0.9997	0.9953	2.0088	0.0317	0.0044	0.0169
3	0.0474	0.9996	– 0.8849	0.2691	0.9996	0.9925	2.0143	0.0468	0.0071	0.0276
4	0.0476	0.9993	– 0.8091	0.2502	0.9993	0.9927	2.0133	0.0467	0.0066	0.0251
5	0.0501	0.9993	– 0.8152	0.2582	0.9993	0.9922	2.0142	0.0492	0.0071	0.0269
6	0.0636	0.999	– 0.787	0.2813	0.999	0.9898	2.0184	0.0622	0.0091	0.0335
7	0.0598	0.9994	– 0.8655	0.2952	0.9994	0.9901	2.0186	0.059	0.0092	0.0335
8	0.2287	0.9967	– 0.8239	0.5236	0.9967	0.948	2.0973	0.2241	0.0463	0.1784
9	0.13	0.9973	– 0.7389	0.3759	0.9973	0.976	2.0426	0.1262	0.0209	0.078
10	0.13	0.9973	- 0.7389	0.3759	0.9973	0.976	2.0426	0.1262	0.0209	0.078
11	0.1136	0.998	– 0.779	0.3673	0.998	0.9793	2.0374	0.1108	0.0184	0.0695
12	0.1026	0.998	– 0.7488	0.3399	0.998	0.982	2.032	0.0998	0.0157	0.0589
13	0.1013	0.9979	– 0.7416	0.3354	0.9979	0.9823	2.0313	0.0984	0.0154	0.0574
14	0.113	0.9979	– 0.7681	0.3625	0.9979	0.9795	2.0368	0.1101	0.0181	0.0681
15	0.1522	0.997	– 0.7573	0.4115	0.997	0.9705	2.0531	0.148	0.0258	0.0973
16	0.1054	0.9982	– 0.7807	0.3553	0.9982	0.9811	2.0342	0.1029	0.0168	0.0635
17	0.058	0.9995	- 0.8886	0.2976	0.9995	0.9904	2.0184	0.0574	0.0091	0.0354
18	0.0609	0.9994	– 0.8616	0.2969	0.9994	0.9899	2.0189	0.0601	0.0094	0.0363
19	0.0585	0.9992	– 0.8052	0.2754	0.9992	0.9907	2.017	0.0574	0.0084	0.032
20	0.0643	0.9992	– 0.8261	0.2941	0.9992	0.9894	2.0195	0.0631	0.0096	0.0369

Table 6 Feature extraction of MS-free dataset

Sl. no.	Autocorrelation	Cluster prominence	Cluster shade	Contrast	Correlation	Difference entropy	Difference variance	Dissimilarity	Energy
1	1.8026	1.2847	0.724	0.003	0.9925	0.0202	0.003	0.003	0.605
2	1.7628	1.3004	0.7407	0.0029	0.9923	0.02	0.0029	0.0029	0.617
3	1.8009	1.2754	0.7183	0.007	0.9822	0.0416	0.0069	0.007	0.601
4	1.692	1.29	0.742	0.0134	0.9624	0.0712	0.0133	0.0134	0.629
5	1.8669	1.2537	0.6887	0.0032	0.9923	0.0215	0.0032	0.0032	0.585
6	1.7026	1.2846	0.7378	0.0148	0.9591	0.077	0.0146	0.0148	0.624
7	1.8477	1.2633	0.7002	0.0032	0.9921	0.0216	0.0032	0.0032	0.591
8	1.8308	1.272	0.7099	0.003	0.9926	0.0203	0.003	0.003	0.596
9	1.4108	1.1807	0.6667	0.0111	0.9535	0.0611	0.011	0.0111	0.75
10	1.5036	1.2878	0.7367	0.0032	0.9887	0.0214	0.0032	0.0032	0.717
11	1.5261	1.2755	0.7326	0.0105	0.9639	0.0584	0.0104	0.0105	0.698
12	1.6836	1.2946	0.7453	0.0122	0.9655	0.0659	0.0121	0.0122	0.634
13	1.9701	1.1907	0.6095	0.006	0.9863	0.0366	0.006	0.006	0.556
14	2.0582	1.1464	0.5345	0.0025	0.9945	0.0174	0.0025	0.0025	0.541
15	2.03	1.163	0.5618	0.0024	0.9947	0.0168	0.0024	0.0024	0.547
16	1.9922	1.1852	0.5961	0.0023	0.9948	0.0163	0.0023	0.0023	0.555
17	1.9654	1.2008	0.6188	0.0023	0.9946	0.0166	0.0023	0.0023	0.561
18	1.9229	1.2255	0.6522	0.0022	0.9948	0.0159	0.0022	0.0022	0.572
19	1.8499	1.2643	0.7003	0.0023	0.9942	0.0165	0.0023	0.0023	0.591
20	1.6643	1.3222	0.7628	0.0033	0.9905	0.0221	0.0033	0.0033	0.651

(continued)

Table 6 (continued)

Sl. no.	Entropy	Homogeneity	Information measure of correlation 1	Information measure of correlation 2	Inverse difference	Maximum probability	Sum average	Sum entropy	Sum of squares variance	Sum variance
1	0.6011	0.9985	−0.9659	0.8214	0.9985	0.7305	2.536	0.5991	0.1962	0.0469
2	0.5871	0.9985	−0.9654	0.8159	0.9985	0.7438	2.5095	0.5851	0.1898	0.0169
3	0.6221	0.9965	−0.9299	0.8129	0.9965	0.7284	2.5363	0.6173	0.1962	0.0276
4	0.6117	0.9933	−0.873	0.7825	0.9933	0.7604	2.4658	0.6024	0.1787	0.0251
5	0.6229	0.9984	−0.9648	0.8288	0.9984	0.7089	2.579	0.6207	0.2057	0.0269
6	0.6217	0.9926	−0.8638	0.782	0.9926	0.756	2.4733	0.6115	0.1807	0.0335
7	0.6171	0.9984	−0.9644	0.8265	0.9984	0.7153	2.5662	0.6149	0.203	0.0335
8	0.6105	0.9985	−0.9662	0.8249	0.9985	0.7211	2.5549	0.6084	0.2005	0.1784
9	0.4596	0.9944	−0.8587	0.7066	0.9944	0.8557	2.2775	0.4519	0.1195	0.078
10	0.4738	0.9984	−0.9549	0.7611	0.9984	0.83	2.3368	0.4716	0.14	0.078
11	0.5225	0.9947	−0.8811	0.7489	0.9947	0.8176	2.3542	0.5152	0.1458	0.0695
12	0.6029	0.9939	−0.8817	0.7833	0.9939	0.764	2.4598	0.5945	0.177	0.0589
13	0.6664	0.997	−0.9425	0.8337	0.997	0.6726	2.6487	0.6622	0.2192	0.0574
14	0.6667	0.9988	−0.9733	0.8471	0.9988	0.6456	2.7063	0.665	0.2284	0.0681
15	0.6601	0.9988	−0.9741	0.8453	0.9988	0.6551	2.6874	0.6585	0.2256	0.0973
16	0.6512	0.9988	−0.9745	0.8426	0.9988	0.6677	2.6622	0.6496	0.2215	0.0635
17	0.6449	0.9988	−0.9739	0.8402	0.9988	0.6766	2.6444	0.6433	0.2184	0.0354
18	0.6332	0.9989	−0.9746	0.8366	0.9989	0.6909	2.616	0.6316	0.2131	0.0363
19	0.6127	0.9988	−0.9727	0.8286	0.9988	0.7151	2.5674	0.611	0.2032	0.032
20	0.5509	0.9984	−0.9594	0.7987	0.9984	0.7764	2.4439	0.5486	0.1727	0.0369

Table 7 Final Result

Classification model	Accuracy (%)	Loss function (%)
Convolutional neural network	98	4

6 Conclusion

The intelligent computer aided diagnosis system for brain tumor segmentation is proposed in this research work. The data of 61 IBSR tumored magnetic resonance imagining and 40 MR-free non-tumored data is considered and observed. The fusion of OTSU embedded adaptive particle swarm optimization is used for obtaining the best threshold value to be applied for segmentation. The automatic brain tumor segmentation is performed involving skull stripping technique. The 19 statistical and texture features are extracted using GLCM which are used in training of convolutional neural network. The categorial cross entropy loss function, RELu and SoftMax activation function is taken in convolutional neural network. Convolutional neural network contributed in improving the classification results of adopted methodology by achieving the accuracy of 98% which is better than other existing system. In future the model will be designed for different modalities of data and other metaheuristic algorithm can be used for improving the performance of the diagnosed system.

Acknowledgements Authors would like to thank for the support and valuable time provided by Amity university, Noida

References

1. Roy S, Bandyopadhyay SK (2012) Detection and quantification of brain tumor from MRI of brain and it's symmetric analysis. Int J Inf Commun Technol Res 2(6)
2. McAuliffe MJ, Lalonde FM, McGarry D, Gandler W, Csaky K, Trus BL (2001) Medical image processing, analysis and visualization in clinical research. In: Proceedings 14th IEEE symposium on computer-based medical systems. CBMS 2001. IEEE, pp 381–386
3. Despotović I, Goossens B, Philips W (2015) MRI segmentation of the human brain: challenges, methods, and applications. Comput Math Methods Med 2015
4. Zaitoun NM, Aqel MJ (2015) Survey on image segmentation techniques. Proc Comput Sci 65:797–806
5. Mirjalili S, Lewis A (2016) The whale optimization algorithm. Adv Eng Softw 95:51–67
6. Tang YG, Liu D, Guan XP (2007) Fast image segmentation based on particle swarm optimization and two-dimension Otsu method. Control Decis 22(2):202
7. Li L, Sun L, Guo J, Han C, Zhou J, Li S (2017) A quick artificial bee colony algorithm for image thresholding. Information 8(1):16
8. Samantaa S, Dey N, Das P, Acharjee S, Chaudhuri SS (2013) Multilevel threshold based gray scale image segmentation using cuckoo search. arXiv:1307.0277
9. Soffer S, Ben-Cohen A, Shimon O, Amitai MM, Greenspan H, Klang E (2019) Convolutional neural networks for radiologic images: a radiologist's guide. Radiology, 290(3):180547

10. Li Q, Cai W, Wang X, Zhou Y, Feng DD, Chen M (2014). Medical image classification with convolutional neural network. In: 2014 13th international conference on control automation robotics & vision (ICARCV), December 2014. IEEE, pp 844–848
11. Schmidhuber J (2015) Deep learning in neural networks: an overview. Neural Netw 61:85–117
12. Suzuki K (2017) Overview of deep learning in medical imaging. Radiol Phys Technol 10(3):257–273
13. Erickson BJ, Korfiatis P, Akkus Z, Kline TL (2017) Machine learning for medical imaging. Radiographics 37(2):505–515
14. Sutskever I, Vinyals O, Le QV (2014) Sequence to sequence learning with neural networks. In: Advances in neural information processing systems, pp 3104–3112
15. Tajbakhsh N, Shin JY, Gurudu SR, Hurst RT, Kendall CB, Gotway MB, Liang J (2016) Convolutional neural networks for medical image analysis: full training or fine tuning? IEEE Trans Med Imaging 35(5):1299–1312
16. Lee JG, Jun S, Cho YW, Lee H, Kim GB, Seo JB, Kim N (2017) Deep learning in medical imaging: general overview. Korean J Radiol 18(4):570–584
17. Lo SCB, Chan HP, Lin JS, Li H, Freedman MT, Mun SK (1995) Artificial convolution neural network for medical image pattern recognition. Neural Netw 8(7–8):1201–1214
18. Litjens G, Kooi T, Bejnordi BE, Setio AAA, Ciompi F, Ghafoorian M, Sánchez CI (2017) A survey on deep learning in medical image analysis. Med Image Anal 42:60–88
19. LeCun Y, Kavukcuoglu K, Farabet C (2010) Convolutional networks and applications in vision. In: Proceedings of 2010 IEEE international symposium on circuits and systems, May 2010. IEEE, pp 253–256
20. Talo M, Baloglu UB, Yıldırım Ö, Acharya UR (2019) Application of deep transfer learning for automated brain abnormality classification using MR images. Cogn Syst Res 54:176–188
21. Balafar MA, Ramli AR, Saripan MI, Mashohor S (2010) Review of brain MRI image segmentation methods. Artif Intell Rev 33(3):261–274
22. Villanueva-Meyer JE, Chang P, Lupo JM, Hess CP, Flanders AE, Kohli M (2019) Machine learning in neurooncology imaging: from study request to diagnosis and treatment. Am J Roentgenol 212(1):52–56
23. Kheirollahi M, Dashti S, Khalaj Z, Nazemroaia F, Mahzouni P (2015) Brain tumors: special characters for research and banking. Adv Biomed Res 4
24. Bauer S, Wiest R, Nolte LP, Reyes M (2013) A survey of MRI-based medical image analysis for brain tumor studies. Phys Med Biol 58(13):R97
25. Drevelegas A, Papanikolaou N (2011) Imaging modalities in brain tumors. In Imaging of brain tumors with histological correlations. Springer, Berlin, pp 13–33
26. Roslan R, Jamil N, Mahmud R (2011) Skull stripping magnetic resonance images brain images: region growing versus mathematical morphology. Int J Comput Inf Syst Ind Manag Appl 3:150–158
27. Ségonne F, Dale AM, Busa E, Glessner M, Salat D, Hahn HK, Fischl B (2004) A hybrid approach to the skull stripping problem in MRI. Neuroimage 22(3):1060–1075
28. Patel J, Doshi K (2014) A study of segmentation methods for detection of tumor in brain MRI. Adv Electron Electr Eng 4(3):279–284
29. Park JG, Lee C (2009) Skull stripping based on region growing for magnetic resonance brain images. NeuroImage 47(4):1394–1407
30. Ahmmed R, Swakshar AS, Hossain MF, Rafiq MA (2017). Classification of tumors and it stages in brain MRI using support vector machine and artificial neural network. In: 2017 International conference on electrical, computer and communication engineering (ECCE), February. IEEE, pp 229–234
31. Cabria I, Gondra I (2017) MRI segmentation fusion for brain tumor detection. Inf Fusion 36:1–9
32. Ayachi R, Amor NB (2009). Brain tumor segmentation using support vector machines. In: European conference on symbolic and quantitative approaches to reasoning and uncertainty, July 2009. Springer, Berlin, pp 736–747

33. Soleimani V, Vincheh FH (2013). Improving ant colony optimization for brain MRI image segmentation and brain tumor diagnosis. In: 2013 first Iranian conference on pattern recognition and image analysis (PRIA), March 2013. IEEE, pp 1–6
34. Jothi G (2016) Hybrid Tolerance Rough Set-Firefly based supervised feature selection for MRI brain tumor image classification. Appl Soft Comput 46:639–651
35. Manic KS, Priya RK, Rajinikanth V (2016) Image multithresholding based on Kapur/Tsallis entropy and firefly algorithm. Indian J Sci Technol 9(12):89949
36. Sharma M, Purohit GN, Mukherjee S (2018) Information retrieves from brain MRI images for tumor detection using hybrid technique K-means and artificial neural network (KMANN). In: Networking communication and data knowledge engineering. Springer, Singapore, pp 145–157
37. Jafari M, Shafaghi R (2012) A hybrid approach for automatic tumor detection of brain MRI using support vector machine and genetic algorithm. Glob J Sci engineering and Technol 3:1–8
38. Jiang J, Trundle P, Ren J (2010) Medical image analysis with artificial neural networks. Comput Med Imaging Graph 34(8):617–631
39. Goodband JH, Haas OCL, Mills JA (2008) A comparison of neural network approaches for on-line prediction in IGRT. Med Phys 35(3):1113–1122
40. Lo SC, Li H, Freedman MT (2003) Optimization of wavelet decomposition for image compression and feature preservation. IEEE Trans Med Imaging 22(9):1141–1151
41. Suzuki K, Horiba I, Sugie N (2003) Neural edge enhancer for supervised edge enhancement from noisy images. IEEE Trans Pattern Anal Mach Intell 25(12):1582–1596
42. Havaei M, Davy A, Warde-Farley D, Biard A, Courville A, Bengio Y, Larochelle H (2017) Brain tumor segmentation with deep neural networks. Med Image Anal 35:18–31
43. Gao XW, Hui R, Tian Z (2017) Classification of CT brain images based on deep learning networks. Comput Methods Progr Biomed 138:49–56
44. Pereira S, Pinto A, Alves V, Silva CA (2016) Brain tumor segmentation using convolutional neural networks in MRI images. IEEE Trans Med Imaging 35(5):1240–1251
45. Sharma A, Kumar S, Singh SN (2018) Brain tumor segmentation using DE embedded OTSU method and neural network. Multidimens Syst Signal Process 30(3):1263–1291
46. Mohan G, Subashini MM (2018) MRI based medical image analysis: survey on brain tumor grade classification. Biomed Signal Process Control 39:139–161
47. Chen H, Dou Q, Yu L, Qin J, Heng PA (2018) VoxResNet: deep voxelwise residual networks for brain segmentation from 3D MR images. NeuroImage 170:446–455
48. Zhao X, Wu Y, Song G, Li Z, Zhang Y, Fan Y (2018) A deep learning model integrating FCNNs and CRFs for brain tumor segmentation. Med Image Anal 43:98–111
49. Kumar V, Sachdeva J, Gupta I, Khandelwal N, Ahuja CK (2011) Classification of brain tumors using PCA-ANN. In: 2011 world congress on information and communication technologies, December 2011. IEEE, pp 1079–1083
50. Lashkari A (2010) A neural network based method for brain abnormality detection in MR images using Gabor wavelets. Int J Comput Appl 4(7):9–15
51. Wang G, Li W, Ourselin S, Vercauteren T (2017) Automatic brain tumor segmentation using cascaded anisotropic convolutional neural networks. In: International MICCAI brainlesion workshop, September 2017. Springer, Cham, pp 178–190
52. Byale H, Lingaraju GM, Sivasubramanian S (2018) Automatic segmentation and classification of brain tumor using machine learning techniques. Int J Appl Eng Res 13(14):11686–11692
53. Kharrat A, Gasmi K, Messaoud MB, Benamrane N, Abid M (2010) A hybrid approach for automatic classification of brain MRI using genetic algorithm and support vector machine. Leonardo J Sci 17(1):71–82
54. Ortiz A, Górriz JM, Ramírez J, Salas-Gonzalez D, Llamas-Elvira JM (2013) Two fully-unsupervised methods for MR brain image segmentation using SOM-based strategies. Appl Soft Comput 13(5):2668–2682
55. Shanthi KJ, Sasikumar MN, Kesavadas C (2010) Neuro-fuzzy approach toward segmentation of brain MRI based on intensity and spatial distribution. J Med Imaging Radiat Sci 41(2):66–71

56. El Abbadi NK, Kadhim NE (2017) Brain cancer classification based on features and artificial neural network. Brain 6(1)
57. El-Dahshan ESA, Hosny T, Salem ABM (2010) Hybrid intelligent techniques for MRI brain images classification. Digit Signal Process 20(2):433–441
58. Gibson E, Li W, Sudre C, Fidon L, Shakir DI, Wang G, Whyntie T (2018) NiftyNet: a deep-learning platform for medical imaging. Comput Methods Progr Biomed 158:113–122
59. Akkus Z, Galimzianova A, Hoogi A, Rubin DL, Erickson BJ (2017) Deep learning for brain MRI segmentation: state of the art and future directions. J Digit Imaging 30(4):449–459
60. Shen D, Wu G, Suk HI (2017) Deep learning in medical image analysis. Annu Rev Biomed Eng 19:221–248
61. Kamnitsas K, Ledig C, Newcombe VF, Simpson JP, Kane AD, Menon DK, Glocker B (2017) Efficient multi-scale 3D CNN with fully connected CRF for accurate brain lesion segmentation. Med Image Anal 36:61–78
62. Zhao L, Jia K (2015) Deep feature learning with discrimination mechanism for brain tumor segmentation and diagnosis. In: 2015 international conference on intelligent information hiding and multimedia signal processing (IIH-MSP), September 2015. IEEE, pp 306–309
63. Nie D, Wang L, Gao Y, Sken D (2016). Fully convolutional networks for multi-modality isointense infant brain image segmentation. In: 2016 IEEE 13th international symposium on biomedical imaging (ISBI), April 2016. IEEE, pp 1342–1345
64. Li Q et al (2014) Medical image classification with convolutional neural network. In: 2014 13th international conference on control automation robotics & vision (ICARCV). IEEE
65. Chao J et al (2019) CaRENets: compact and resource-efficient CNN for homomorphic inference on encrypted medical images. arXiv:1901.10074
66. Loizou CP, Petroudi S, Seimenis I, Pantziaris M, Pattichis CS (2015) Quantitative texture analysis of brain white matter lesions derived from T2-weighted MR images in MS patients with clinically isolated syndrome. J Neuroradiol 42(2):99–114
67. http://www.medinfo.cs.ucy.ac.cy/
68. Zhuang AH, Valentino DJ, Toga AW (2006) Skull-stripping magnetic resonance brain images using a model-based level set. NeuroImage 32(1):79–92
69. Zhan ZH, Zhang J, Li Y, Chung HSH (2009) Adaptive particle swarm optimization. IEEE Trans Syst Man Cybern Part B (Cybern) 39(6):1362–1381
70. Duraisamy SP, Kayalvizhi R (2010) A new multilevel thresholding method using swarm intelligence algorithm for image segmentation. J Intell Learn Syst Appl 2(03):126
71. Sezgin M, Sankur B (2004) Survey over image thresholding techniques and quantitative performance evaluation. J Electron Imaging 13(1):146–166
72. Ker J, Wang L, Rao J, Lim T (2018) Deep learning applications in medical image analysis. IEEE Access 6:9375–9389
73. Hore A, Ziou D (2010). Image quality metrics: PSNR vs. SSIM. In: 2010 20th international conference on pattern recognition, August 2010. IEEE, pp 2366–2369
74. Yeghiazaryan V, Voiculescu I (2015) An overview of current evaluation methods used in medical image segmentation. Technical report CS-RR-15–08 Department of Computer Science, University of Oxford, Oxford, UK
75. Jain A, Zongker D (1997) Feature selection: Evaluation, application, and small sample performance. IEEE Trans Pattern Anal Mach Intell 19(2):153–158
76. Malegori C, Franzetti L, Guidetti R, Casiraghi E, Rossi R (2016) GLCM, an image analysis technique for early detection of biofilm. J Food Eng 185:48–55
77. Zayed N, Elnemr HA (2015) Statistical analysis of haralick texture features to discriminate lung abnormalities. J Biomed Imaging 2015:12